Inhibition of factor-dependent transcription termination in *Escherichia coli* might relieve xenogene silencing by abrogating H-NS-DNA interactions *in vivo*

DEEPTI CHANDRAPRAKASH and ASWIN SAI NARAIN SESHASAYEE

National Centre for Biological Sciences, Tata Institute of Fundamental Research, GKVK, Bellary Road, Bangalore 560 065, India

**Corresponding author (Email, aswin@ncbs.res.in)*

Many horizontally acquired genes (xenogenes) in the bacterium *Escherichia coli* are maintained in a silent transcriptional state by the nucleoid-associated transcription regulatory protein H-NS. Recent evidence has shown that antibiotic-mediated inhibition of the transcription terminator protein Rho leads to de-repression of horizontally acquired genes, akin to a deletion of *hns*. The mechanism behind this similarity in outcomes between the perturbations of two distinct processes remains unclear. Using ChIP-seq of H-NS in wild-type cells, in addition to that in cells treated with bicyclomycin – a specific inhibitor of Rho, we show that bicyclomycin treatment leads to a decrease in binding signal for H-NS to the *E. coli* chromosome. Rho inhibition leads to RNA polymerase readthrough, which in principle could displace H-NS from the DNA, thus leading to transcriptional derepression of H-NS-silenced genes. Other possible mediators of the effect of Rho on H-NS are discussed. A possible positive feedback between Rho and H-NS might help reinforce xenogene silencing.

[Chandraprakash D and Seshasayee ASN 2014 Inhibition of factor-dependent transcription termination in *Escherichia coli* might relieve xenogene silencing by abrogating H-NS-DNA interactions *in vivo*. *J. Biosci.* **39** 53–61] **DOI**10.1007/s12038-014-9413-4

1. Introduction

H-NS is a nucleoid-associated protein, which regulates transcription in *Escherichia coli* and related bacteria. It is primarily a transcription silencer, which binds to A+T-rich sequences and/or intrinsically bent DNA (Dorman 2007). It forms either stiff rods (Liu *et al.* 2010b) or DNA-H-NS-DNA bridges (Dame *et al.* 2006), both of which might be indicative of gene silencing. Many horizontally acquired genes (referred to as 'xenogenes') in *E. coli* and other enterobacteria are A+T-rich in sequence (for example, Kahramanoglou *et al.* 2011), and therefore are maintained in a silent transcriptional state by H-NS. A corollary of these facts is that the deletion of *hns* leads to large-scale transcriptional up-regulation of A+T-rich xenogenes.

The function of H-NS is modulated by multiple other proteins, including DNA binding proteins such as the H-NS homolog StpA and the LysR family protein LeuO, and oligomerization-promoting proteins such as Hha and YdgT (Stoebel *et al.* 2008). In addition, there is evidence that inhibition of the transcription terminator Rho causes an increase in the expression of horizontally acquired genes (Cardinale *et al.* 2008), among other functions (Peters *et al.* 2009). Later investigations showed explicitly that many genes which are transcriptionally upregulated by Rho inhibition are also bound by H-NS on the chromosome (Peters *et al.* 2012). Further, there is a synthetic negative genetic interaction between *hns* and *rho* (Peters *et al.* 2012).

What are the mechanisms that establish this unexpected similarity between the transcriptional effects of a DNA-binding nucleoid-associated protein and those of a transcription terminator? A genetic study by Saxena and Gowrishankar (2011) showed that defects in Rho-

Keywords. Gene silencing; hns; horizontal gene transfer; transcription termination; rho

Supplementary materials pertaining to this article are available on the *Journal of Biosciences* Website at: *http://www.ias.ac.in/jbiosci/mar2014/supp/Chandraprakash.pdf*

Published online: 27 January 2014

dependent transcription termination can be suppressed by over-expression of YdgT, a protein that is homologous to the oligomerization domain of H-NS. Similar suppression was also seen with certain mutations in the H-NS oligomerization domain itself. This suggested a model in which the oligomeric H-NS filaments on the chromosome alter the properties of the transcription elongation complex such that it becomes more susceptible to termination by Rho. A similar direct effect of H-NS on Rho-dependent termination has also been proposed by Peters, Landick and co-workers (Peters *et al.* 2012). It has been shown that transcriptional repression of *bglG* by H-NS binding 600-700 bp downstream of the transcription start site requires Rho-dependent transcription termination (Dole *et al.* 2004b). This suggested to the authors again that H-NS might be a roadblock to the RNA polymerase, and that this might promote Rho-dependent transcription termination; however, it is not clear that this rules out the converse where Rho-dependent termination helps regulate H-NS-DNA interactions. Having H-NS and Rho regulate each other would infact impose a positive feedback, which would help reinforce gene silencing when switched on.

A popular genome-scale technique for interrogating protein-DNA interactions *in vivo* is Chromatin immunoprecipitation followed by deep sequencing (ChIP-seq) (Liu *et al.* 2010a). This is a state-of-the-art alternative to ChIP-chip, in which a microarray is used in place of deep sequencing. Both these techniques have been used to investigate H-NS-DNA interactions in *E. coli* and *Salmonella enterica Typhimurium* (Lucchini *et al.* 2006; Oshima *et al.* 2006; Kahramanoglou *et al.* 2011). In the present study, in contrast to models implicating H-NS as a regulator of Rho function, we used ChIP-seq to test whether Rho would in fact influence H-NS-DNA interactions.

2. Materials and methods

2.1 *Strain construction and general growth conditions*

The bacterial strain used in this work is *Escherichia coli* K12 MG1655 CGSC6300. The *hns* gene in this strain was C-terminally tagged with the sequence encoding the 3xFLAG epitope using the λ Red recombinase (Datsenko and Wanner 2000) – based method of Uzzau *et al.* (2001). The kanamycin cassette inserted thus was removed by FLP-mediated site-specific recombination. Luria broth was used for normal growth. Where needed, Bicyclomycin (BCM, a generous gift from the Max Gottesman laboratory) was used to a final concentration of 25 μg mL^{-1}, previously used by Cardinale and colleagues (Cardinale *et al.* 2008) in generating the gene expression profile of *E. coli* in the presence of BCM.

2.2 *Chromatin immunoprecipitation and deep sequencing*

ChIP was performed, in two biological replicates for BCM+ and BCM− samples, in a manner similar to that reported previously (Kahramanoglou *et al.* 2011). A more detailed protocol is described in Supplementary Methods. Prior to sequencing, quality of the DNA was checked using Bioanalyzer and Qubit. Libraries for sequencing were prepared using the kit from NEB (Cat#:E6200L, Cat#:6240 L, Cat#:E7500L, Cat#:E7335L), and multiplexed sequencing was performed for 50 cycles from one end on an Illumina HiSeq 1000 system.

2.3 *Real-time qPCR*

To measure the enrichment of H-NS binding sites in the immunoprecipitated DNA samples, real-time quantitative PCR was performed. 3 ng of ChIP sample or the input DNA control, specific primers against binding regions identified in our ChIP-seq experiments and Power SYBR Green PCR master mix (Applied Biosystems Cat #: 4367659) were used for the reaction.

2.4 *Data analysis*

Reads obtained after Illumina sequencing were aligned to the reference genome of *E. coli* K12 MG1655 using the Burrows-Wheeler aligner (BWA) (Li and Durbin 2009), using a quality threshold of 20 (-q 20 option in bwa aln command). After alignment, all reads that had mapped to more than one locus were discarded. Overall >95% of the reads had aligned to a single site on the reference genome. The SAM file output from BWA lists, for each read, the mapped position as the left-most coordinate of the alignment. This position was extended to 280 bp, equal to the average length of DNA fragments submitted for sequencing. For each coordinate, the coverage was calculated as the number of reads, which had aligned against that position. This distribution is shown in supplementary figure 1.

The coverage was normalized and converted into a z-score as described previously (Kahramanoglou *et al.* 2011). The normalisation ensures that the mode of the normalized coverage distribution – assumed to reflect the background – is close to zero for all samples, independent of the sequencing coverage. The z-score distributions for the samples used in the study are given in supplementary figure 2. A z-score threshold of 12 was selected to identify H-NS binding regions. This threshold gave a similar number of enriched sites in the BCM− condition as described in our previous H-NS ChIP-seq study. In the input DNA sequencing, hardly any position crossed this threshold. The binding regions were defined as described previously

(Kahramanoglou *et al.* 2011), by considering every base position with a z-score greater than the defined threshold, and merging adjacent binding regions separated by a distance of less than 200 bp into a single binding region.

Binding regions consistently identified in two samples were defined as those where at least 50% of the binding region in one of the two samples overlapped with a single binding region from the other. From these overlap profiles, a consensus binding region was defined as that portion which was covered by both the samples in the comparison.

The results showing a decrease in H-NS binding signal in BCM+ when compared to BCM− were based on the average z-scores between two biological replicates. However, one replicate appeared to produce consistently weaker signals than the other. Supplementary figure 3 presents a comparison of BCM+ and BCM− using binding regions identified in the BCM− replicate producing the weaker signals (replicate 2), and comparing these ChIP-signals with those from the BCM+ replicate producing the stronger signals (replicate 1).

RNA-seq data for wildtype *E. coli* K12 MG1655, grown in LB to mid-exponential phase, were obtained from our previous work (Srinivasan *et al.* 2013), and normalized and processed as described in the above work. The only difference being that the expression measure was calculated for consecutive, non-overlapping bins of 200 bp each, unaware of gene annotations, whereas in the previous study the measure was calculated for each mRNA gene.

2.5 *Data availability*

All data have been submitted to the NCBI Gene Expression Omnibus, with the accession number GSE51582.

3. Results

We performed a ChIP-seq investigation of H-NS in *E. coli* (K12 MG1655 CGSC6300) grown in the rich Luria broth, in the presence or absence of the antibiotic bicyclomycin (BCM) – a specific inhibitor of Rho (Zwiefka *et al.* 1993; Kohn and Widger 2005). We refer to the untreated samples as BCM− and the BCM-treated samples as BCM+. For these experiments, H-NS was tagged with a 3xFLAG epitope on the chromosome using homologous recombination (Uzzau *et al.* 2001), and an anti-FLAG antibody used for immunoprecipitation. The ChIP was performed as per previously published protocols (Kahramanoglou *et al.* 2011), with specific modifications described in the supplementary material. Immunoprecipitated DNA fragments from both BCM+ and BCM− cells were subjected to high-throughput Illumina sequencing, on a HiSeq1000 model. In addition, matched input DNA fragments were also sequenced as controls. Millions of 50-mer sequencing reads were mapped to the *E. coli* K12 MG1655 genome, and the number of reads mapping to each base position on the genome calculated.

An inspection of the histogram of read counts across the genome showed the presence of a sharp peak on the left of the distribution, representing the background (supplementary figure 1). A long tail on the right corresponds to regions of read count enrichment, i.e. loci preferentially immunoprecipitated by the antibody. The read counts were normalized using a method described earlier for ChIP-seq data for *E. coli* (Kahramanoglou *et al.* 2011), which converts read counts into z-scores against the inferred background distribution. The right skew of the read count distributions was maintained in the z-score distributions, except that the mode of the distributions were all now close to zero instead of being dependent on the sequencing coverage (figure 1; supplementary figure 2). Although the right skew is consistent across all the ChIP samples, with little to no right-tail in the input control, it is clear that the skew is considerably more pronounced in BCM− than in BCM+. This is reflected in the skewness measure, which is ~4.6-4.7 for the two BCM− replicates, and ~2.9-3.2 for the two BCM+ replicates.

Using the z-score scheme, we identified H-NS binding regions in our data for BCM− (figure 2a). The two biological replicates used in this study agreed with each other. Although the binding signal is consistently weaker in one replicate, as many as 92 % of the binding regions in this replicate were also identified independently in the other. None of these binding regions showed any significant signal in the input control. These binding regions were in excellent agreement with previous ChIP-seq data produced by Kahramanoglou *et al.* (2011). Over 95 % of the binding regions identified in both the BCM− replicates overlapped with binding regions identified in the earlier study. This is despite the fact that the Kahramanoglou study, which involved one of the present authors, was performed in a different laboratory and in a slightly different variant of *E. coli* K12 MG1655 (Freddolino *et al.* 2011).

For each binding region thus identified in BCM−, we calculated a ChIP-signal score, which was defined by the average of the base-level z-scores across the length of the binding region. This score was computed for the binding regions in both BCM− and BCM+. Examination of the scatter plot of the signals for BCM+ against BCM− revealed a massive drop in the ChIP signal for H-NS in BCM+ (figure 2b; supplementary figure 3). This difference is greater than what we observe as the difference between two biological replicates for BCM+or BCM−. Despite the large difference in H-NS binding signal between BCM− and BCM+, there is a reasonable linear correlation between the two (Pearson's correlation coefficient ~0.6), indicating that

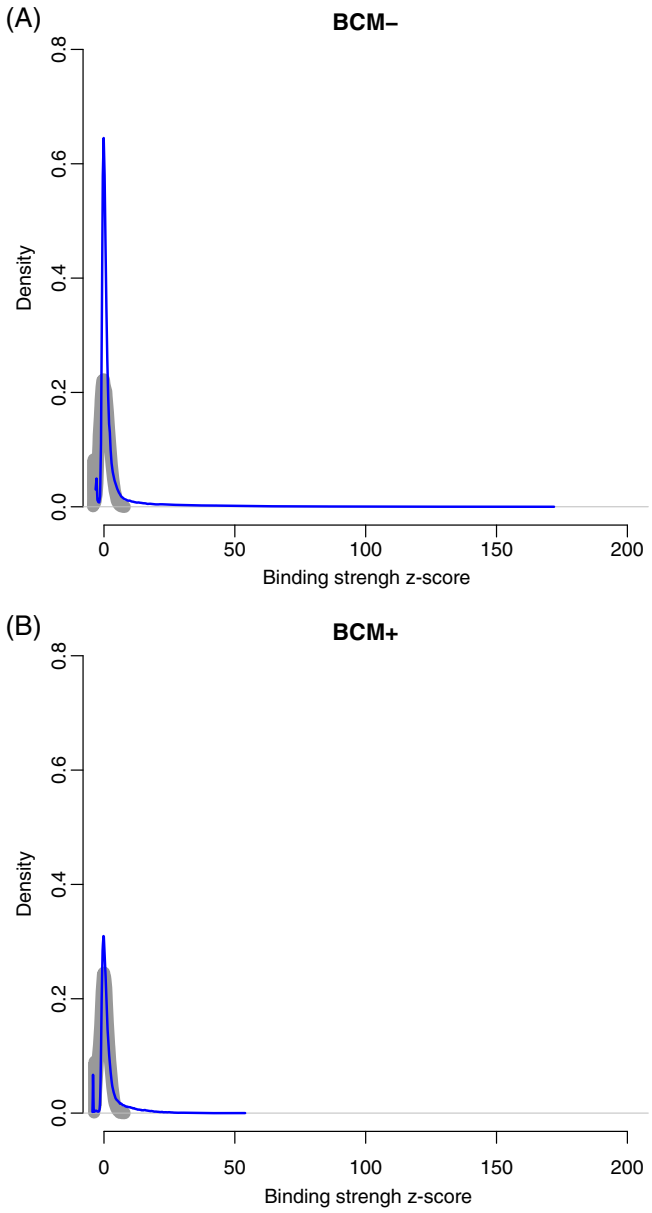

Figure 1. The figure shows a density distribution of the z-scores obtained from the ChIP-seq experiments for H-NS (blue) and the corresponding input DNA sample (thick grey curves), for (**A**) BCM− and (**B**) BCM+. 50-mer reads were aligned to the reference genome of *E. coli* K12 MG1655 using the program BWA (Li and Durbin 2009; Cardinale *et al.* 2008). The mapped position, which represents the left end of the alignment, was extended to 280 bp, which is the average length of DNA fragments used for sequencing. The number of reads aligning to each base position was computed. To account for differences between samples in sequencing coverage, the above numbers were converted into z-scores against the presumed distribution of the background, as described earlier (Kahramanoglou *et al.* 2011). For this purpose, the *genefilter* package in R was used. The distributions shown here represent the average z-scores between two biological replicates.

some H-NS binding signal has been recovered in BCM+ as well. In a second type of analysis, we identified H-NS binding regions in BCM+ (figure 2a), for subsequent comparison with those identified in BCM−. Whereas ~475 H-NS binding regions were consistently identified in the two BCM− samples, only ~315 were so identified across the two BCM+ replicates. Most (82 %) of the BCM+ H-NS binding regions are also present in BCM−. In line with the general decrease in the binding signal for H-NS in BCM+, the binding regions identified in BCM+ are considerably shorter than the corresponding regions in BCM− (figure 2c).

A potential pitfall of this study is the possibility that different ChIP experiments might produce different signal-to-noise (S/N) ratios (Shao *et al.* 2012), as a result of experimental artifacts. Computational techniques, which account for such differences are not applicable to the present data. This is because these techniques assume that most binding regions that are common to two samples have similar binding signals (Shao *et al.* 2012), whereas we appear to see a global reduction in H-NS binding in BCM+ when compared to BCM− cells. However, the following points argue against the chance that artifactual global differences in S/N ratios could account for our results: All the above-described experiments were performed in parallel by the same individual (DC) and using the same batch of antibody, thus minimizing person-to-person variability in protocol execution and lot-to-lot variation in reagents. Secondly, the S/N ratio difference between BCM+ and BCM− samples is much greater than that between replicates. It has even been suggested that S/N ratio variation may not be a major issue when comparing multiple conditions for the same cell type using the same antibody (Bardet *et al.* 2012).

To further establish that the differences we observe are real, we performed the following analyses: We performed two additional ChIPs starting from stored frozen pellets from each of the two BCM+ and BCM− samples (technical replication of the ChIP experiment on the same batch of cells). Experimental artifacts causing unreliable decrease in S/N ratios are unlikely to be carried over to additional replicate ChIPs. Following the ChIP, enrichments in signal for a few H-NS binding regions were tested using qPCR. We observed once again that the H-NS binding signal was considerably weaker for BCM+ than for BCM− (supplementary figure 4). We also observed that H-NS ChIPs from BCM+ appeared to pull down less DNA product than those from BCM−, although the two did not differ from each other in the total input DNA yield (supplementary figure 5). Finally, we performed two mock-IP-seq experiments, one for each treatment. We noticed no difference between BCM− and BCM+ mock-IP signals over the H-NS binding regions, suggesting that there is no systematic *en masse* difference in background pulldown efficiency between the two samples (supplementary figure 6).

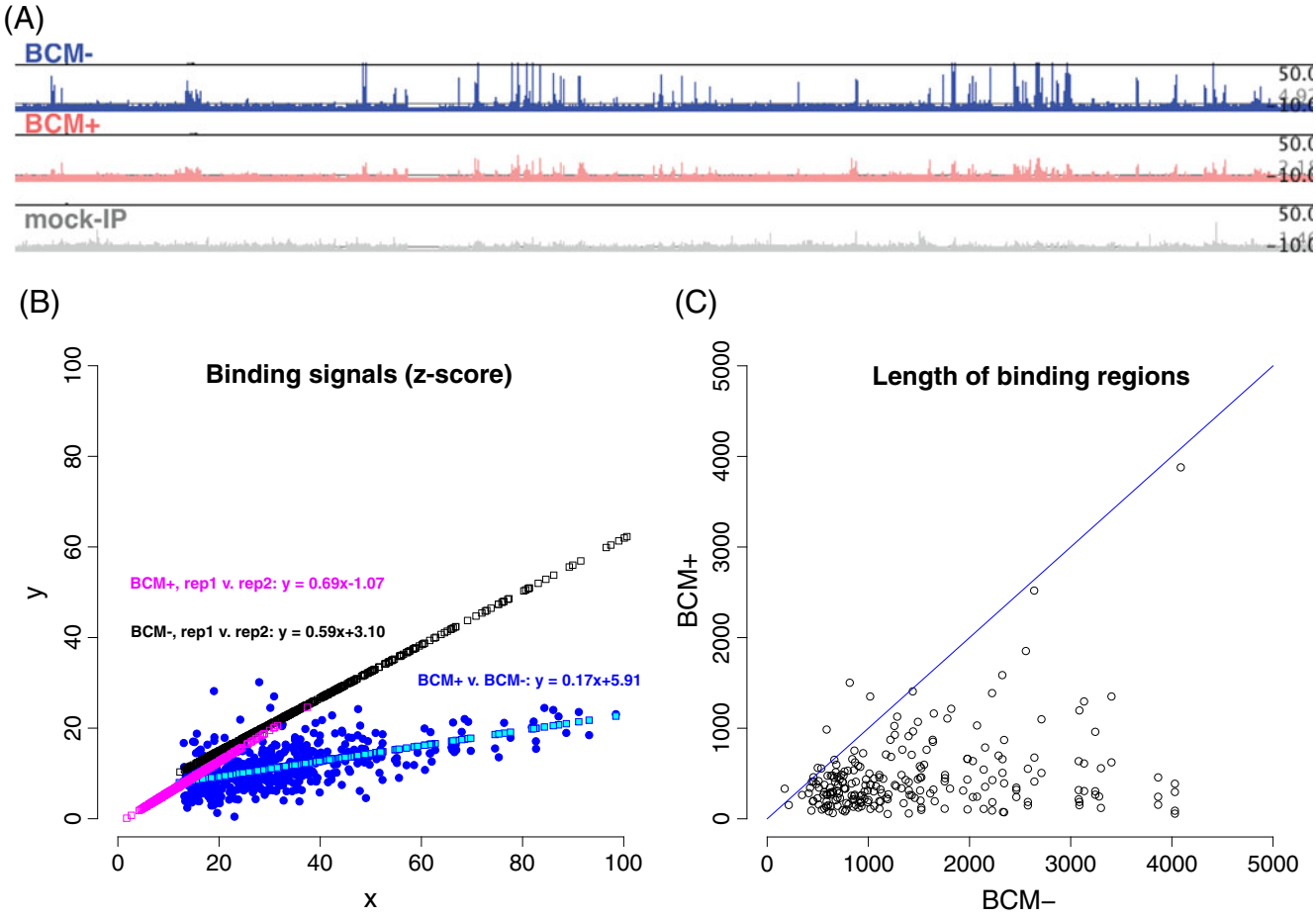

Figure 2. (**A**) Genome browser tracks showing ChIP signals for BCM− (blue), BCM+ (light red) and a mock-IP (grey), over a randomly picked stretch covering ~10 % of the *E. coli* K12 MG1655 genome. All three tracks are drawn on the same y-axis scale. (**B**) The panel shows a scatter plot (filled blue circles) of the binding signals for BCM+ (y-axis) and BCM− (x-axis) within binding regions consistently identified in both BCM− replicates (see supplementary material). The average z-scores between replicates were used to plot the graph. The cyan squares show the linear regression fit between BCM+ and BCM− binding signals. The unfilled black and magenta squares show the regression fit between the two replicates for BCM− and BCM+ respectively. The regression equations are also marked in the corresponding colours. (**C**) This panel shows a scatter plot of the length of binding regions identified in both BCM+ and BCM− samples. Each binding region represented here was recovered across replicates and across conditions. The 45° line is marked.

4. Discussion

Our analyses indicate that inhibition of Rho by treatment with BCM might abrogate H-NS binding to the chromosome across most of its binding regions, if not all. In other words, the effect of BCM treatment on H-NS-DNA interactions is global. These results suggest a foundation for previously reported observations that bicyclomycin-sensitive transcripts also tend to be bound by H-NS (Peters *et al.* 2012). The factors which lead to the enrichment of A+T-rich xenogenes among BCM-sensitive transcripts remain unknown, unless H-NS itself regulates Rho activity globally as posited elsewhere (Saxena and Gowrishankar 2011; Peters *et al.* 2012). Our data neither support nor contradict this hypothesis. However, we note that regulation of Rho by H-NS – alongside the converse that we report here – would imply a positive feedback between Rho and H-NS, which when switched on will reinforce xenogene silencing. The mechanism behind the effect of Rho on H-NS is not clear, and we speculate on various testable hypotheses below.

4.1 *RNA polymerase readthrough as a possible mediator of the effect of Rho inhibition on H-NS-DNA interactions*

Although this remains to be shown, RNA polymerase readthrough in the absence of a fully functional Rho might displace H-NS from the chromosome. This is not too farfetched. Firstly, from RNA-seq data for *E. coli* grown in

LB (Srinivasan *et al.* 2013), we observe that genomic regions immediately adjacent to H-NS binding regions – but not marked as bound by H-NS – are expressed at levels similar to any average gene on the chromosome (figure 3). Therefore, there is RNA polymerase activity around H-NS binding regions, although not within them. Secondly, optical tweezer experiments have shown that a 7pN force is sufficient to break a DNA-H-NS-DNA bridge at a DNA unwinding rate similar to that of the RNA polymerase (Dame *et al.* 2006; Stoebel *et al.* 2008). The movement of RNA polymerase during transcription could generate a force of up to 25pN (Wang *et al.* 1998; Stoebel *et al.* 2008), considerably more than what is required to displace H-NS. This model is illustrated in figure 4. Additionally, there is evidence that transcriptional roadblocks imposed by various DNA binding proteins can be cleared, even close to the transcription initiation site, by a train of RNA polymerase molecules passing through (Epshtein *et al.* 2003).

To analyse further the effect of transcription from surrounding loci on H-NS binding, we computed the fold-change in binding score between BCM− and BCM+. There was a correlation between the fold change and the strength of binding of H-NS in BCM− cells. This effect was normalized by linear regression, and the residuals (FC^R) taken as a measure of the magnitude of the effect of bicyclomycin (Rho inhibition) on H-NS-DNA interactions. An FC^R of 0 indicates that the fold change in binding strength between BCM− and BCM+ is what is expected given the BCM− binding strength; $FC^R<0$ implies a fold change that is less than expected and; $FC^R>0$ represents a fold change greater than expected. In summary, smaller the FC^R, less is the effect of BCM on H-NS-DNA interactions. Overall, there is not much variation in the normalized effect across binding regions, suggesting that the degree of loss of H-NS-DNA interactions is largely uniform. However, we notice a very weak correlation ($\rho=0.10$) between FC^R and the expression levels of loci surrounding the H-NS binding region. This number corresponds to a borderline statistical significance ($P=0.056$), compared to a null model in which the association between gene expression and FC^R is shuffled (supplementary figure 7). In fact, for binding regions surrounded by loci of low gene expression, FC^R has a slight tendency to be below zero ($P=0.02$; Wilcoxon test; supplementary figure 7), whereas those adjacent to loci of higher expression display no such trend ($P=0.41$; Wilcoxon test). Additionally, we also tested for association between gene expression within a H-NS binding region in a Δ*hns-stpA* strain (Srinivasan *et al.* 2013) – which lacks H-NS and its homolog StpA – and found that loci that are highly expressed (top one-third among binding regions; RNA-seq data) in this strain tend to show higher FC^R than those with low expression (bottom one-third; $P=0.0003$; Wilcoxon test; supplementary figure 8). This might speculatively suggest that increased expression

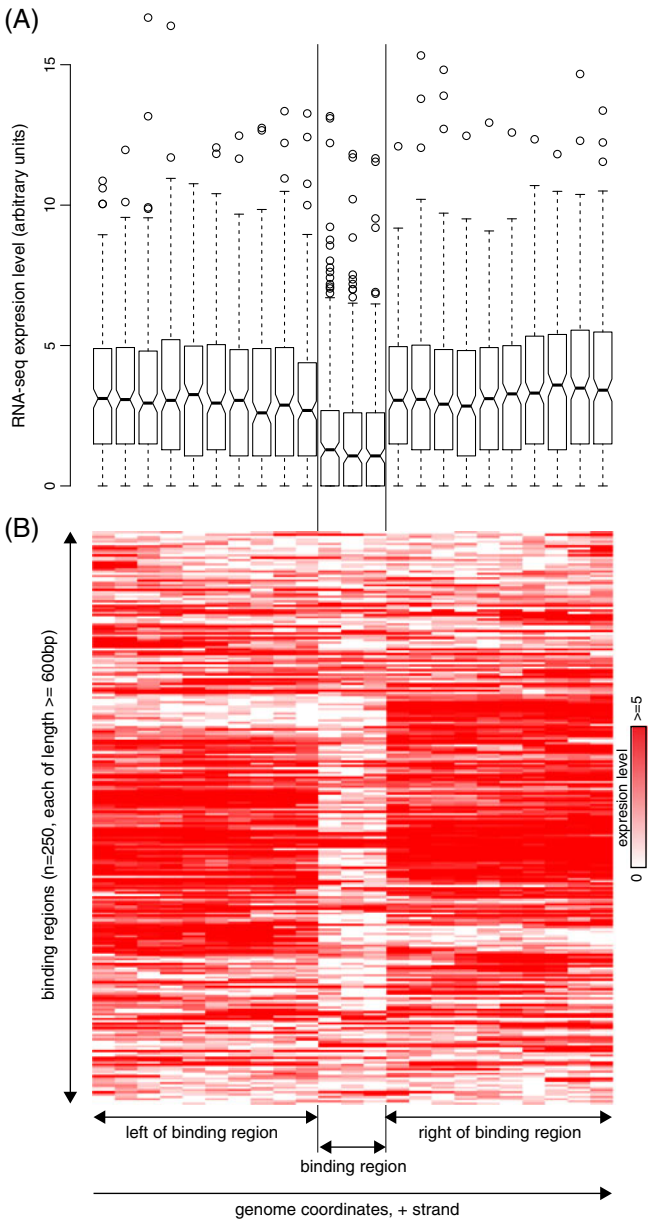

Figure 3. Each H-NS binding region of length ≥ 600 bp (arbitrary) was divided into three bins of 200 bp each (for longer binding regions, the central 600 bp were used), and 10 bins of the same size on either side of the binding region were considered. For each of these bins, an expression measure was computed from previously-published data for *E. coli* grown to mid-exponential phase in LB medium (Srinivasan *et al.* 2013). (**A**) This panel shows the distribution of the gene expression measures for each of the bins across ~250 H-NS binding regions. (**B**) This panel shows the expression measure for each binding region and the bins surrounding it in the form of a heat map, with binding regions listed down the vertical, and genomic coordinates relative to the centre of the binding region along the horizontal. In this heat map, red stands for high expression levels, and white for low expression levels or transcriptional silencing.

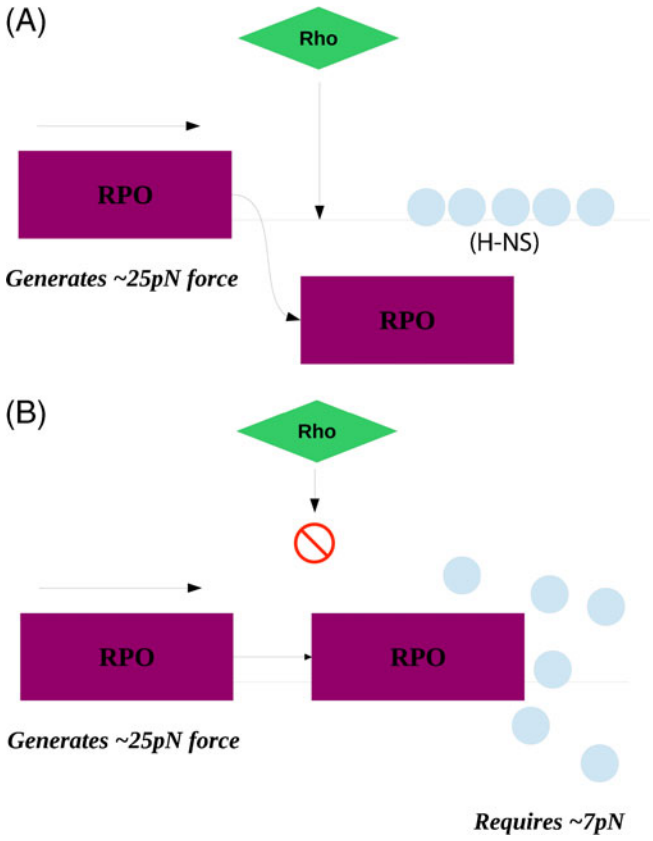

Figure 4. A working model for the interaction between Rho and H-NS. (**A**) A schematic representation of transcription termination by Rho ensuring that H-NS stays bound to the DNA; (**B**) when Rho is inhibited, RNA polymerase readthrough might displace H-NS from its binding sites. The forces mentioned in this figure were obtained from a review (Stoebel *et al.* 2008). The green diamonds represent Rho, the magenta rectangles show the RNA polymerase and the light blue circles stand for H-NS. We note that the previously proposed model of H-NS regulating Rho function (Saxena and Gowrishankar 2011; Peters *et al.* 2012) would impose a positive feedback on this circuit, thus reinforcing gene silencing.

following displacement of H-NS from the chromosome might be a barrier to the protein rebinding to its site.

Taken together, these arguments suggest that there is a weak association between the effect of Rho inhibition on H-NS-DNA interactions, and the expression levels of loci surrounding H-NS binding regions. These might be supportive of the model wherein RNA polymerase readthrough displaces H-NS from its binding sites. The fact that the correlation is weak might emerge from the conclusions of previous studies showing that a train of two cooperating RNA polymerases is sufficient to break transcriptional roadblocks (Epshtein *et al.* 2003); this might in fact be reflected in the largely uniform FC^R across the genome. Such fine distinctions at the level of single RNA polymerase molecules might be difficult to observe in the population-averaged and coarse-grained genome-scale data described here.

4.2 *Supercoiling as a possible second intermediary between Rho and H-NS*

A second possible effector for the impact of Rho inhibition on H-NS-DNA interactions is the effect of the former on DNA supercoiling. It has been previously shown that a mutant (*rho-15*) allele of *rho* induces DNA relaxation (Fassler *et al.* 1986). However, whether the negative influence of DNA relaxation on H-NS-DNA interactions will be strong enough, across the entire genome, to explain our observations is debatable. There is a statistically significant overlap (Scolari *et al.* 2012) between the set of relaxation-induced genes determined by gene expression microarrays (Peter *et al.* 2004) and H-NS-bound genes (Kahramanoglou *et al.* 2011). However, this accounts for only ~6% of H-NS targets, in contrast to our results showing an effect on nearly every H-NS binding region on the chromosome. Our previous ChIP-seq study (Kahramanoglou *et al.* 2011) of H-NS did not observe any reduction of H-NS-DNA interactions during stationary phase, where the DNA is more relaxed than in exponential phase. A recent study in *Salmonella* did not find any evidence for DNA relaxation having an impact on H-NS binding to selected promoters (Cameron and Dorman 2012).

4.3 *4.3 Other intermediaries*

There are several other possible intermediaries between Rho and H-NS. Does Rho inhibition decrease H-NS levels? There is no evidence to suggest that it does. The transcriptome studies of Peters *et al.* (2012) do not show a decrease in *hns* expression level following bicyclomycin treatment. Although there is an increase in antisense transcription from the H-NS locus, antisense transcripts seem to be expressed at much lower levels than sense transcripts, and whether these are sufficient to have any significant negative effect on the expression of their corresponding sense transcripts is debatable. H-NS is not among the list of proteins that showed differential expression between BCM− and BCM+ in a proteomic study by Cardinale and colleagues (Cardinale *et al.* 2008).

Finally, H-NS also binds to RNA. This is based on evidence that it interacts with the *rpoS* and the *dsrA* mRNA (Brescia *et al.* 2004). Pervasive transcription introduced by Rho inhibition might titrate out H-NS, thus leaving little protein available for interactions with the DNA. This is suggestive. However, at this point, the number of RNA molecules to which H-NS binds is not known, and therefore the extent of the ability of the RNA-binding activity of H-NS to abrogate its interactions with the DNA remains to be tested.

An additional factor, which is involved in the Rho-H-NS interplay is the RNA-binding chaperone Hfq, which has been shown to promote anti-termination at Rho-dependent terminators by forming a complex with Rho (Rabhi *et al.* 2011). There is genetic evidence that mutations in *hfq* release H-NS-mediated silencing of the *bgl* operon (Dole *et al.* 2004a), alongside the evidence that Rho is necessary for efficient H-NS-dependent silencing of this locus (Dole *et al.* 2004b). An early genetic study has shown that *hfq* is a multicopy suppressor of the effect of Δ*hns* on the expression of the arginine decarboxylase gene (Shi and Bennett 1994). The genome-wide effects of this three-way interaction *in vivo* remains to be systematically tested.

5. Conclusion

Therefore, irrespective of whether the intermediary is RNA polymerase readthrough or DNA relaxation or titration of H-NS by RNA, the loss of H-NS-DNA interactions might be an immediate cause of the transcriptional de-repression of xenogenes observed in bicyclomycin-treated *E. coli* (Cardinale *et al.* 2008). The possible mechanisms behind the effect of Rho on H-NS, in the face of cellular complexity and the combinatorial control of H-NS-mediated repression (Stoebel *et al.* 2008), are possibly best tested *in vitro*.

Our result, in the context of RNA polymerase roadblocks, also suggests the importance of transcription termination in efficient repression of transcription initiation by H-NS. A positive feedback between Rho and H-NS – based on models suggesting the regulation of Rho activity by H-NS – might reinforce xenogene silencing.

Acknowledgements

Research on H-NS in our laboratory is supported by NCBS core funding, the Ramanujan Fellowship (SR/S2/RJN-49/2010) to ASNS and a research grant (SB/SO/BB-0073/2012) from the Department of Science and Technology, India. We thank Professor Max Gottesman and his laboratory for giving us a generous gift of bicyclomycin, without which this study would not have been possible. We thank Professors Georgi Muskhelishvili and Sankar Adhya for their comments and suggestions on this work. We thank Professor J Gowrishankar for discussions that introduced us to this problem. We also thank the anonymous referees for comments, which helped us improve our original manuscript considerably. Library preparation and sequencing were performed at the Next Generation Genomics Laboratory at the Centre for Cellular and Molecular Platforms (C-CAMP), who trialled the NEB ChIP library preparation kit for this study.

References

Bardet AF, He Q, Zeitlinger J and Stark A 2012 A computational pipeline for comparative ChIP-seq analyses. *Nat. Protoc.* **7** 45–61

Brescia CC, Kaw MK and Sledjeski DD 2004 The DNA binding protein H-NS binds to and alters the stability of RNA in vitro and in vivo. *J. Mol. Biol.* **339** 505–514

Cameron ADS and Dorman CJ 2012 A fundamental regulatory mechanism operating through OmpR and DNA topology controls expression of Salmonella pathogenicity islands SPI-1 and SPI-2. *PLoS Genet.* **8** e1002615

Cardinale CJ, Washburn RS, Tadigotla VR, *et al.* 2008 Termination factor Rho and its cofactors NusA and NusG silence foreign DNA in *E. coli. Science* **320** 935–938

Dame RT, Noom MC and Wuite GJL 2006 Bacterial chromatin organization by H-NS protein unravelled using dual DNA manipulation. *Nature* **444** 387–390

Datsenko KA and Wanner BL 2000 One-step inactivation of chromosomal genes in Escherichia coli K-12 using PCR products. *Proc. Natl. Acad. Sci. USA* **97** 6640–6645

Dole S, Klingen Y, Nagarajavel V and Schnetz K 2004a The protease Lon and the RNA-binding protein Hfq reduce silencing of the Escherichia coli bgl operon by H-NS. *J. Bacteriol.* **186** 2708–16

Dole S, Nagarajavel V and Schnetz K 2004b The histone-like nucleoid structuring protein H-NS represses the Escherichia coli bgl operon downstream of the promoter. *Mol. Microbiol.* **52** 589–600

Dorman CJ 2007 H-NS, the genome sentinel. *Nat. Rev. Microbiol.* **5** 157–61

Epshtein V, Toulmé F, Rahmouni AR, *et al.* 2003 Transcription through the roadblocks: the role of RNA polymerase cooperation. *EMBO J.* **22** 4719–4727

Fassler JS, Arnold GF and Tessman I 1986 Reduced superhelicity of plasmid DNA produced by the rho-15 mutation in *Escherichia coli. MGG Mol. Gen. Genet.* **204** 424–429

Freddolino PL, Amini S and Tavazoie S 2011 Newly identified genetic variations in common MG1655 stock cultures. *J. Bacteriol.* doi: 10.1128/JB.06087-11

Kahramanoglou C, Seshasayee ASN, Prieto AI, *et al.* 2011 Direct and indirect effects of H-NS and Fis on global gene expression control in *Escherichia coli. Nucleic Acids Res.* **39** 2073–2091

Kohn H and Widger W 2005 The molecular basis for the mode of action of bicyclomycin. *Curr. Drug Targets Infect. Disord.* **5** 273–295

Li H and Durbin R 2009 Fast and accurate short read alignment with Burrows-Wheeler transform. *Bioinformatics* **25** 1754–1760

Liu ET, Pott S and Huss M 2010a Q&A: ChIP-seq technologies and the study of gene regulation. *BMC Biol.* **8** 56

Liu Y, Chen H, Kenney LJ and Yan J 2010b A divalent switch drives H-NS/DNA-binding conformations between stiffening and bridging modes. *Genes Dev.* **24** 339–344

Lucchini S, Rowley G, Goldberg MD, *et al.* 2006 H-NS mediates the silencing of laterally acquired genes in bacteria. *PLoS Pathog.* **2** e81

Oshima T, Ishikawa S, Kurokawa K, *et al.* 2006 Escherichia coli histone-like protein H-NS preferentially binds to horizontally acquired DNA in association with RNA polymerase. *DNA Res.* **13** 141–153

Peter BJ, Arsuaga J, Breier AM, *et al.* 2004 Genomic transcriptional response to loss of chromosomal supercoiling in *Escherichia coli*. *Genome Biol*. **5** R87

Peters JM, Mooney RA, Grass JA, *et al.* 2012 Rho and NusG suppress pervasive antisense transcription in *Escherichia coli*. *Genes Dev*. **26** 2621–2633

Peters JM, Mooney RA, Kuan PF, *et al.* 2009 Rho directs widespread termination of intragenic and stable RNA transcription. *Proc. Natl. Acad. Sci. USA* **106** 15406–15411

Rabhi M, Espéli O, Schwartz A, *et al.* 2011 The Sm-like RNA chaperone Hfq mediates transcription antitermination at Rho-dependent terminators. *EMBO J*. **30** 2805–2816

Saxena S and Gowrishankar J 2011 Modulation of Rho-dependent transcription termination in Escherichia coli by the H-NS family of proteins. *J. Bacteriol.* **193** 3832–3841

Scolari VF, Zarei M, Osella M and Lagomarsino MC 2012 NuST: analysis of the interplay between nucleoid organization and gene expression. *Bioinformatics* **28** 1643–1644

Shao Z, Zhang Y, Yuan G-C, *et al.* 2012 MAnorm: a robust model for quantitative comparison of ChIP-Seq data sets. *Genome Biol*. **13** R16

Shi X and Bennett GN 1994 Plasmids bearing hfq and the hns-like gene stpA complement hns mutants in modulating arginine decarboxylase gene expression in *Escherichia coli*. *J. Bacteriol.* **176** 6769–6775

Srinivasan R, Chandraprakash D, Krishnamurthi R, *et al.* 2013 Genomic analysis reveals a bi-layered epistatic control of 'expensive' genes in Escherichia coli K-12: implications for gene silencing. *Mol. Biosyst.* doi: 10.1039/c3mb70035f

Stoebel DM, Free A and Dorman CJ 2008 Anti-silencing: overcoming H-NS-mediated repression of transcription in Gram-negative enteric bacteria. *Microbiology* **154** 2533–2545

Uzzau S, Figueroa-Bossi N, Rubino S and Bossi L 2001 Epitope tagging of chromosomal genes in Salmonella. *Proc. Natl. Acad. Sci. USA* **98** 15264–15269

Wang MD, Schnitzer MJ, Yin H, *et al.* 1998 Force and velocity measured for single molecules of RNA polymerase. *Science* **282** 902–907

Zwiefka A, Kohn H and Widger WR 1993 Transcription termination factor rho: the site of bicyclomycin inhibition in Escherichia coli. *Biochemistry* **32** 3564–3570

MS received 18 November 2013; accepted 27 December 2013

Corresponding editor: DURGADAS P KASBEKAR